Downloaded from http://sp.lyellcollection.org/ by guest on December 10, 2018

New results of Boda Claystone research: Genesis, mineralogy, geochemistry, petrophysics

FERENC FEDOR[1]*, ZOLTÁN MÁTHÉ[2], PÉTER ÁCS[1] & PÉTER KORONCZ[1]

[1]*GEOCHEM Ltd, 55/1 Viola str., Kozármisleny, H-7761, Hungary*

[2]*MECSEKÉRC Co., 19. Esztergár L. str., Pécs H-7633, Hungary*

F.F., 0000-0002-1938-9496

**Correspondence: fedor.ferenc@geochem-ltd.eu*

Abstract: Boda Claystone is a very tight clayey rock with extreme low porosity and permeability, nano-size pores and small amounts of swelling clays. Due to this character it is ideal as a potential host rock for research into the possibilities of high-level waste deposition in geological formation. Though the research started more than 30 years ago, the genesis, the geotectonic history of the Boda Claystone Formation (BCF) and the geology of surrounding areas has only been sketched out recently. On the basis of research of the past few years the process of sedimentation of different blocks was able to be reconstructed. Equipment and methodological developments were needed for the investigation of reservoir geological and hydrodynamic behaviour of this rock, which began in the early 2000s. Based on them the pore structure and reservoir could be characterized in detail. Only theoretical approaches were available for the chemical composition of free porewater. Traditional water-extracting methods were not adaptable because of excessively low porosity and nano-scale pore size distribution. Hence, new ways have to be found for getting enough water for analysis. These new results of BCF research help to prepare more sophisticated and directed experiments, in which there is a great interest internationally.

The Upper Permian Boda Claystone Formation (BCF) is located in the Western Mecsek Mountains, Southern Transdanubia, SW Hungary. The Mecsek Mountains are part of the Tisza Megaunit comprising the basement of the south-eastern half of the Pannonian Basin (Haas & Péró 2004). In the Western Mecsek Mountains (WM Mts) the BCF extends over an area of 150 km^2; within this area, approximately15 km^2 can be found on the surface in the Boda village region (Fig. 1). Two distribution areas of the BCF are known in WM Mts (Figs 2 and 3): (1) the peri-anticlinal structure of the WM Mts, named the Boda block, and (2) the so called Gorica block. In the Gorica block outcrop of the BCF it is not on the surface, but several deep drillings have reached it and of these only the borehole Ib-4 has recovered the BCF in significant thickness (494.2–709.0 m).

On the basis of the deep drillings the total thickness of the BCF is estimated to be about 700–900 m in the peri-anticlinal structure of the WM Mts (Boda block), whereas its thickness is smaller in the Gorica block (about 350 m). The BCF is predominantly red and reddish brown in colour, reflecting its predominantly oxidizing nature (Jámbor 1964; Barabás & Barabás-Stuhl 1998; Máthé 1998; Árkai *et al.* 2000; Varga *et al.* 2005; Lázár & Máthé 2012). According to our present-day knowledge, the BCF has only one reduce interbedding (greyish black claystone containing pyrite and finely distributed organic matter), its thickness being about 3–4 m. Lithological sequences of the two areas are shown in Figure 3.

Detailed analysis of the formation has been in progress continuously since the late 80s. The so-called Alpha-tunnel, which operated in mid-1990s was the deepest underground research laboratory (URL) of its age. *In-situ* observations and laboratory analysis of core samples specifically serve mineralogical, geochemical, hydrogeological, geotechnical and aging measurements as well as understanding the tectonic and alteration processes (Kovács 1999*a*, *b*). Only limited petrophysical measurements were carried out because of technological reasons (SZKFI 1990, 1991; MÉV 1993; Csicsák 1999). The development of equipment and methodology for porosity and permeability measurements began in the early 2000s and are in progress with other technical developments like acoustic velocity and electric measurements, and pore characterization (Fedor *et al.* 2008, 2016, 2017; Fedor & Somodi 2010; Fedor 2011*a*, *b*; Koroncz & Fedor 2016).

Petrological analysis and genesis of the Boda and Gorica blocks

Based on the mineralogical investigation by X-ray diffraction (XRD), differential thermal analysis (DTA) and electron microprobe analysis (EMP) the

From: Norris, S., Neeft, E.A.C. & Van Geet, M. (eds) *Multiple Roles of Clays in Radioactive Waste Confinement*. Geological Society, London, Special Publications, **482**,
https://doi.org/10.1144/SP482.13
© 2018 The Author(s). Published by The Geological Society of London. All rights reserved.
For permissions: http://www.geolsoc.org.uk/permissions. Publishing disclaimer: www.geolsoc.org.uk/pub_ethics

Downloaded from http://sp.lyellcollection.org/ by guest on December 10, 2018

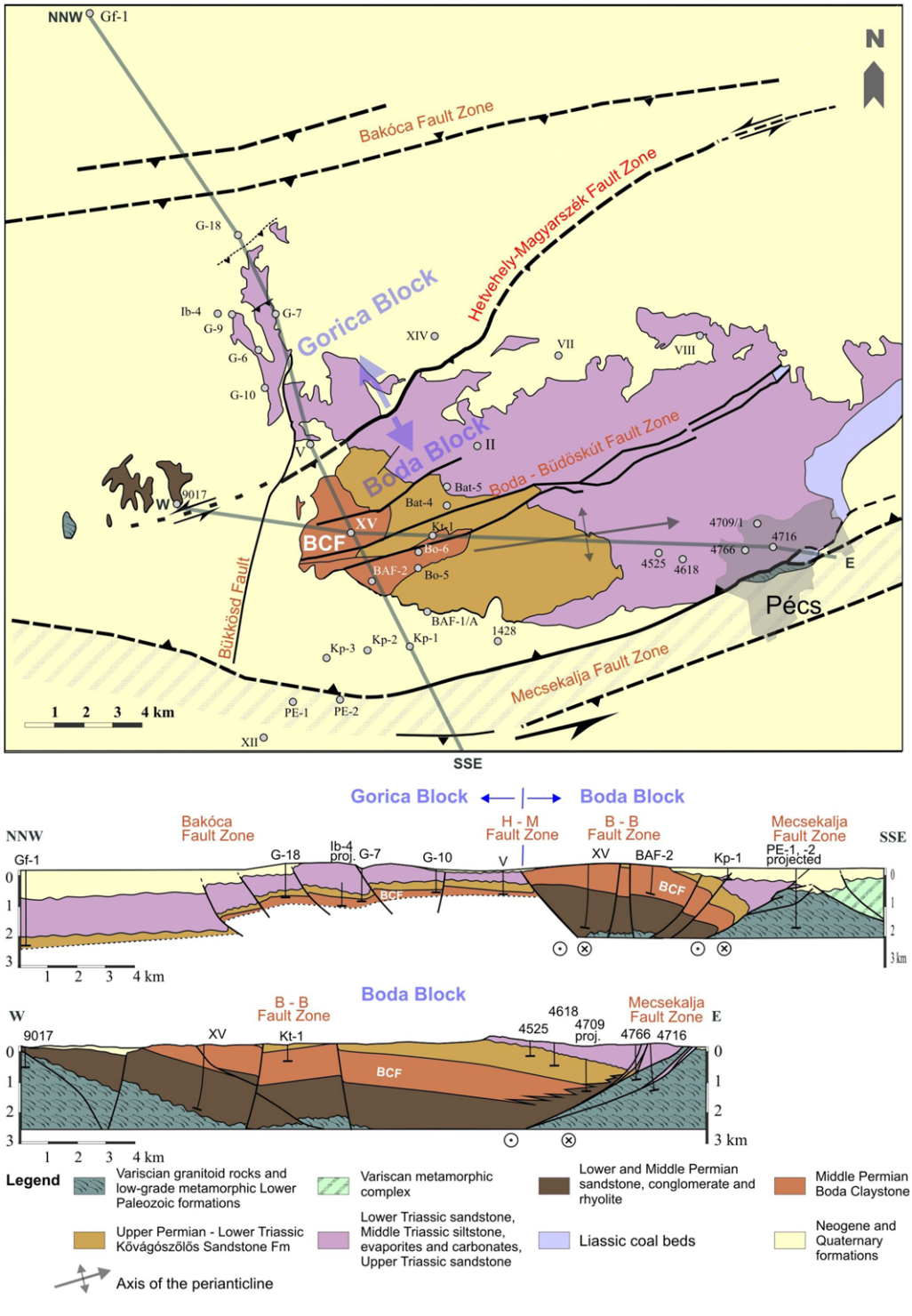


Fig. 1. Geological map and cross sections of the Western Mecsek including the surface outcrop of the BCF (compiled by Konrád in Máthé 2015).

Downloaded from http://sp.lyellcollection.org/ by guest on December 10, 2018

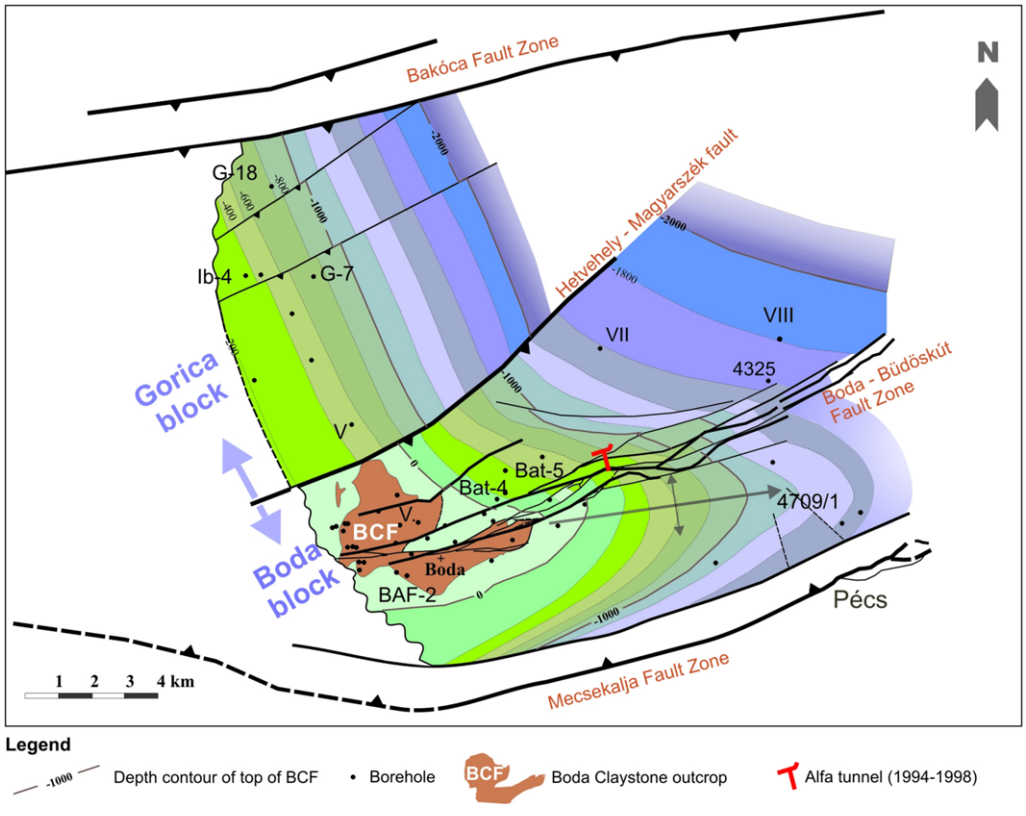


Fig. 2. Depth contour of the top of the BCF including the surface outcrop of the BCF (compiled by Konrád & Hámos in Máthé 2015).

main rock-forming minerals of the BCF in the Boda block are: clay minerals (10–55 wt%), albite (20–60 wt%), detrital quartz (5–30 wt%), carbonate minerals (calcite and dolomite; 10–50 wt%) and hematite (5–10 wt%) (Máthé 1998, 2015; Árkai *et al.* 2000; Varga *et al.* 2005; Varga *et al.* 2006). The absolute dominant clay mineral is illite–muscovite (15–50 wt%), with chlorite (0–35 wt%) as another determinant clay mineral phase; smectite, kaolinite, vermiculite and mixed-layer clay minerals (illite/smectite, chlorite/smectite) being identified in inconsiderable amounts (Máthé 1998, 2015; Árkai *et al.* 2000; Varga *et al.* 2005, 2006). In the greyish-black interstratification the illite–muscovite content decreases, and the chlorite becomes the dominant clay mineral. In the Boda block the most remarkable feature of the BCF is the presence of the abundant albite. Its authigenic genesis is supported by its chemical composition and textural characteristics. The authigenic albite is present as (1) albite cement (typical of all rock types of the BCF), (2) dominantly albite and carbonate-lined disseminated voids, (3) albite replacement of detrital feldspars and (4) a vein of varying thickness containing anhydrite and albite (Máthé 1998, 2015; Árkai *et al.* 2000; Varga *et al.* 2006). The albite and carbonate-lined voids always contain authigenic K-feldspar, with K-feldspar crystals generally filling the centre of the voids, which indicate that this mineral formed after the precipitation of albite. In addition to these rock-forming minerals, barite, anhydrite, pyrite and detrital constituents (muscovite, biotite, chlorite, zircon, rutile, apatite, ilmenite, Ca-bearing plagioclase) were always identified in minor amounts.

In the Gorica block the BCF recovered from the borehole Ib-4 differs in its mineralogical composition, the most significant differences being: (1) this succession of the BCF contains abundant analcime in addition to the above minerals, (2) lack of authigenic K-feldspar and (3) among carbonate phases the amount of dolomite considerably decreases (Sipos *et al.* 2010; Lázár & Máthé 2012; Máthé 2015). Similar to the authigenic albite, the analcime is present as analcime cement and dominantly analcime and carbonate-lined disseminated voids. The amounts of analcime in the BCF grades upward to

Downloaded from http://sp.lyellcollection.org/ by guest on December 10, 2018

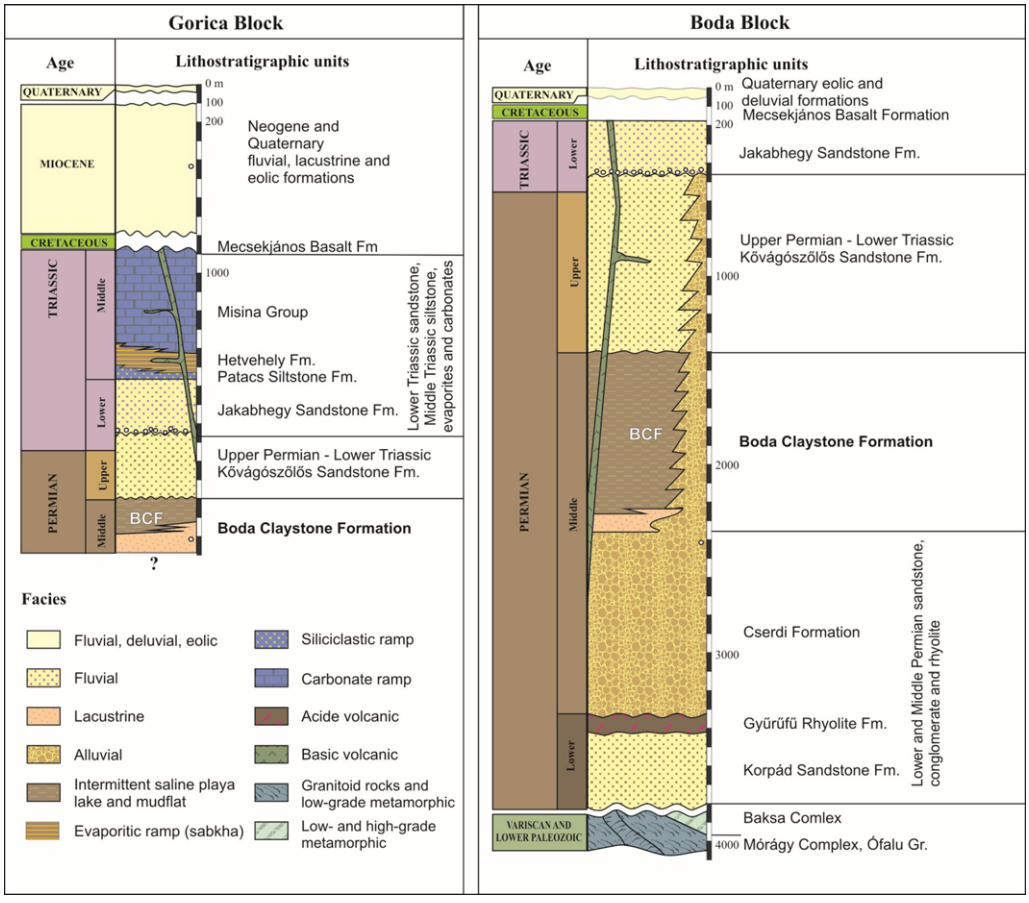


Fig. 3. General geological sections for the comparison of lithostratigraphic units in the Boda and in the Gorica blocks (Konrád 2013).

decrease, the lower third of the formation being analcime free; however, it contains abundant authigenic albite (Máthé 2015).

Based on mineralogical, geochemical and textural considerations five main rock types can be defined in the Boda block: albitic claystone, albitolite, 'true' siltstone, dolomite interbeddings, sandstone. However in the Gorica block it is albite- and analcime-bearing claystone, siltstone and sandstone, dolomite interbeddings being only typical of the upper thin part of the formation (Barabás & Barabás-Stuhl 1998; Máthé 1998, 2015; Árkai *et al.* 2000; Varga *et al.* 2006; Konrád *et al.* 2010; Sipos *et al.* 2010; Lázár & Máthé 2012).

The albitolite presences are massive, hard, unbedded, without any albite and carbonate minerals filling vesicles. Its macroscopic feature is similar to the albitic claystone type of BCF. Albitolite is comprised mostly of authigenic albite (>50 wt%, as albite cement), clay minerals (<25 wt%, generally illite), detrital quartz (10 wt%), carbonate minerals (approx. 10 wt%; calcite and dolomite), hematite (5–6 wt%) (Varga *et al.* 2006; Máthé 2015).

The absolute dominant rock type of the formation is an albitic claystone in the Boda block, whereas the dominant rock type is an albite- and analcime-bearing claystone in the Gorica block.

In the Boda block, illite and chlorite crystallinity, as well as the vitrinite reflectance data, indicate late or deep diagenesis, with a maximum temperature of 200–250°C (Árkai *et al.* 2000; Varga *et al.* 2006). However, in the Gorica block (from core samples of the deep borehole Ib-4) higher illite and chlorite crystallinity indices suggest that the BCF in the Gorica block underwent lower grade diagenesis (Németh *et al.* 2016).

Mineralogical and petrological (dominantly albite, analcime and carbonate-lined voids and

Downloaded from http://sp.lyellcollection.org/ by guest on December 10, 2018

dolomite crystals of dolomite layers are pseudomorphs after 'Hopper halite'; pseudomorphs consisting of authigenic albite and calcite after gypsum and anhydrite; desiccation cracks). Geochemical (e.g. high boron and Na_2O contents) data unambiguously demonstrate the depositional environment of the BCF and the original rock types deposited. According to this evidence the BCF was deposited in shallow-water: halite- and sulphate-dominated, long-lived perennial and ephemeral inland saline lakes surrounded by saline and dry mudflats, and distal alluvial deposits, under semi-arid to arid climatic conditions (Barabás & Barabás-Stuhl 1998; Máthé 1998; Árkai *et al.* 2000; Varga *et al.* 2005; Máthé & Varga 2012). On the other hand, unlike mineralogy, different thicknesses of the two distribution areas of the BCF and textural signatures indicate dissimilar depositional environments.

The thick (700–900 m) red siliciclastic sequence (continental red beds) of the Boda block represent a saline-lake and saline-pan system which is consistent with the model outlined by Lowenstein & Hardie (1985). Their model separates three stages of the saline-pan cycle: (1) flooding, (2) evaporative concentration and (3) desiccation (Fig. 4). During the flooding stage the dissolution surfaces formed, the bedded halite layers and displaced halite crystals in muds and silts dissolved, and the clay, mud, silt and sand layers were deposited in the brackish lake and flooded mudflat. During the evaporative concentration stage, there was precipitation of halite in the saline lake, displaced growth of halite and anhydrite in red sediments of mudflat and dry mudflat, and evaporite crusts formed. The products of the desiccation stage were desiccation cracks in red sediments, microcrystalline salt crusts and displaced halite and anhydrite crystals in sediments. Based on Lowenstein & Hardie's (1985) model and lithologies and sedimentary features of the sequence (continental red beds) of the Boda block, it seems that the original rock types of the sequence of the Boda block were in agreement with the above rock types. The BCF in the Boda block has undergone a multistage and complex diagenetic process (among others primary evaporite minerals dissolved, formation of authigenic albite and K-feldspar, formation of dolomite layers), the result of these multistage processes are present-day mineral assemblages and rock types (Varga *et al.* 2005; Máthé 2015; Németh *et al.* 2016).

In the Gorica block the different minerology (see above) and smaller thickness of the BCF, the absence of dolomite layers, analcime and the irregular form of the analcime and carbonate-lined disseminated voids (not pseudomorphs after halite) suggest that the lake environment in which the formation was deposited was moderately saline and alkaline. The

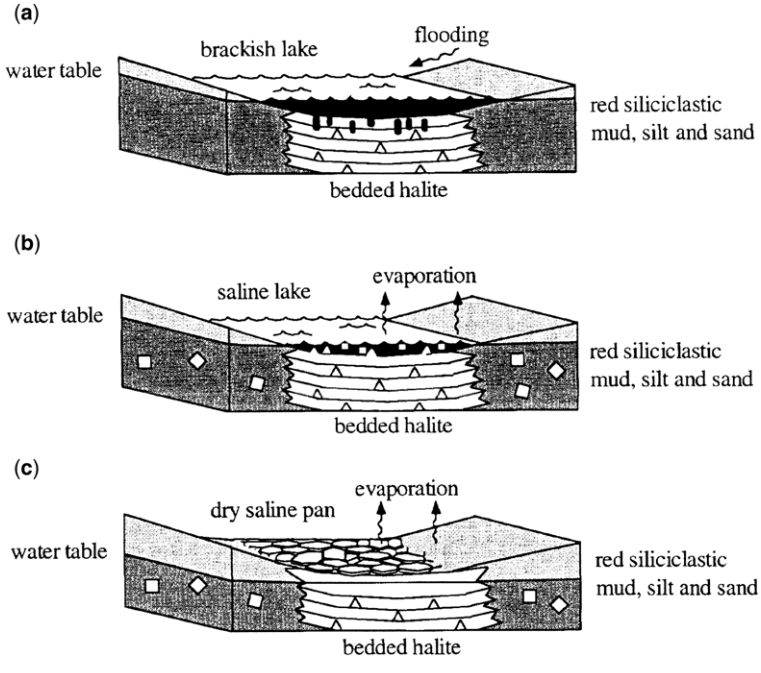


Fig. 4. Schematic models of saline-pan deposition for BCF in the Boda block (Máthé 2015): **(a)** Flooding state; **(b)** evaporative concentration stage; **(c)** desiccation stage.

Downloaded from http://sp.lyellcollection.org/ by guest on December 10, 2018

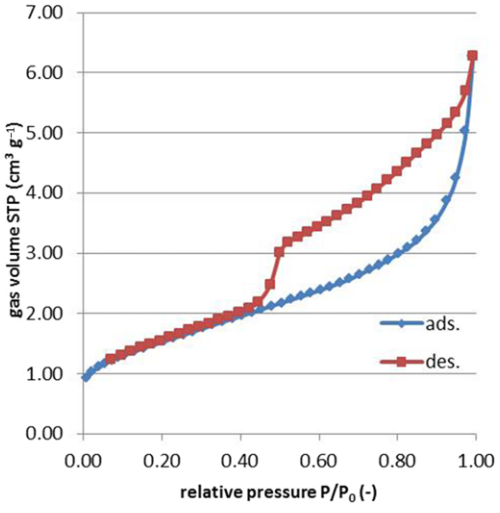


Fig. 5. Adsorption–desorption isotherm of BAF-Ib4 and BAF-2 samples.

Eocene Green River Formation of the south-central Uinta basin (Utah, USA) (Remmy & Ferrell 1989) can be regarded as an ancient analogy for the Gorica BCF analcime-bearing red and green mudstone. The moderately saline and alkaline environment is proved by halite and other evaporite minerals which have been reported neither in the Uinta lake (Remmy & Ferrell 1989) nor in the Gorica lake (Máthé 2015), in addition in neither formation has the analcime altered to potassium feldspar. In both formations evaporative pumping produced the sodium-rich brines on the exposed mudflats. The resulting sodium-rich brine facilitated the formation of analcime by accelerating the alteration of detrital clays,

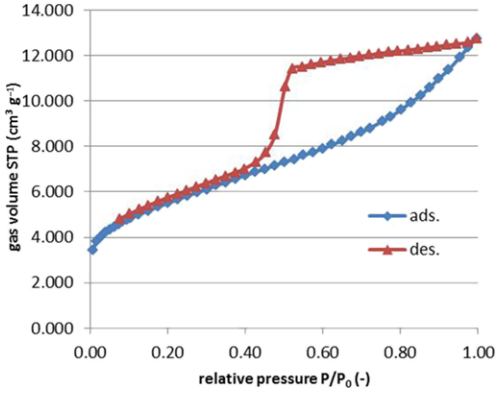


Fig. 6. Adsorption–desorption isotherm of BAF-1, -1A and covering sandstone samples.

and perhaps other minerals, and by providing a source of abundant sodium. Alteration of iron-bearing minerals released iron, which oxidized (formation of Fe-hydroxide or Fe-oxide (perhaps hematite)) consequently staining the mud. In both cases the overall reaction for the formation of analcime is: detrital clays + sodium brine produced by evaporative pumping + iron-bearing minerals + oxygen→ analcime + iron oxide or iron hydroxide (Remmy & Ferrell 1989; Máthé 2015). The smaller proportion of analcime precipitated in pores, occurring as very-fine grained crystals in the matrix, which impregnates the Gorica BCF (Máthé 2015). The Sambhar and Didwana playas from the eastern margin of the Thar Desert (Roy *et al.* 2006) and Lake Lewis, in central Australia (English 2001) can be regarded as recent analogies for Gorica BCF.

Technological challenges of laboratory analysis

The BCF cores from peripheral areas (BAF-1, -1A, -1Af, BAF-2) are more fractured than sampled from central areas (Ib-4, Alpha-tunnel). Drillings of 9, 2.54- and 3.81 mm-diameter and maximum 2″ length plugs from cores are more or less soluble sometimes with the stabilization of core mantle. However, it needs to be considered that intact rock is over-represented during laboratory analysis. Due to developments, nano and pico Darcy scale water permeability and two times higher gas permeability was measurable even under reservoir conditions routinely and reproducibly by RS PPD permeameter (Szűcs & Fedor 2007; Fedor *et al.* 2008). The 0.1–5% porosity could be measured with high accuracy and estimated error (for the given pressure and temperature). A complex protocol was introduced for pore characterization, which includes He-pycnometry, CO_2 and N_2 adsorption–desorption isotherms and Hg-porosimetry measurements for pore surface, pore volume, pore roughness and shape, pore throat-size distribution and porosity calculations in micro (0.3–2 nm), meso (2–50 nm) and macro (>50 nm) scale characterizations (Ács & Fedor 2015). Integration of NMR, which is a promising method for porewater quantity analysis, is only in the first stages.

The measurement of reservoir features is highly important because of geophysical logs interpretation. Basic electric measurements like formation factor or relative permittivity in a given temperature range are routinely fulfilled. However, methodological developments are needed for saturation–desaturation experiments, because the volume of displaced water cannot be measured in a traditional way. The development of multielectrode, wide frequency range-induced polarization tomography and electric resistivity tomography of cores, which is important

Downloaded from http://sp.lyellcollection.org/ by guest on December 10, 2018

for understanding the saturation process in the case of nano-scale pores, is only at the beginning phase. Acoustic wave velocity measurements on dry or saturated cores in triaxial cells with automatic wave analysis for longitudinal (compression) and transverse (shear) waves have already been solved, and hence dynamic rock mechanical parameters like Young's modulus and Poisson's ratio can be calculated for the elastic deformation phase of rocks. Also, Thomsen's anisotropy parameters, which are widely used in depth migration in seismic surveys could be calculated (Koroncz *et al.* 2017). Mechanical parameters have to be handled carefully because of the swelling clays and low-water content of the BCF rock.

Based on neutron porosity logs (H concentration) the estimated amount of water of a typical BCF core sample is *c.* 10–15 vol%, which is partly crystalline water, partly irreducible water in pores (adsorbed water and capillary water trapped in small pores which cannot be removed by drying) and only in small part (1–5%) reducible porewater (water which can be removed by drying). *In-situ* water sampling is impossible on this technological level. Laboratory water sampling and analysis with traditional techniques are also questionable, so methodological development is needed. Finally, neither real water quantity, nor the composition of water is known. It seems that water composition based on theoretical models and equilibrium experiments may in most cases characterize the water of open faults and cracks rather than the real pore structure (Fedor *et al.* 2014).

Pore and reservoir characterization of the BCF

To understand the pore structure and behaviour, detailed petrophysical analysis was carried out including pore structure and reservoir characterization in core samples from Tunnel Alpha (in some Delta-cores; 2002, 2004, 2017) and the boreholes Ib-4 (2009–14, BCF and covering sandstone; Fedor *et al.* 2012; Fedor (ed.) 2013), BAF-1, -1A (did not contain the real BCF) and BAF-2 (2014–15).

Sampling

During the measurements 55 segments of a 10 m long BCF core and 1 m of overlaying sandstone from Ib-4 borehole (Gorica block) were analysed as well as some plugs that were drilled from Delta-3 borehole (Boda block). Axial and horizontal plugs were drilled from the core with 2.54 or 3.81 mm diameter, and fragments were used during the He-pycnometry, Hg-porosimetry and physisorption tests. At this time, the systematic analysis of BAF-1, -1A and BAF-2 samples (Boda block) had been completed (Table 1).

Sample preparation and handling

Laboratory protocols were developed for core analysis. Ultra-pure water was used for cooling during drilling and after drying the samples were immediately put into the desiccator. Rubber gloves were used for touching the samples and humidity and temperature were controlled in the laboratory. On the basis of DTA analysis there is no crystalline change in the BCF up to a couple of hundred °C, so drying at 105°C was used to facilitate porewater removal. When saturation was needed, for example, by reservoir measurements, ultra-pure water was applied for this purpose. However, this protocol is very strict and seemed excessive in the case of natural rock, but in the case of the BCF very small differences can cause large problems during interpretation.

Methods

After drilling and detailed documentation (description and photo) the geometric volume (V_{med}) of the plugs was calculated as a median of 11 independent length and diameter data for each. The samples were dried at 105°C in a drying oven for 12–14 (sometimes more) days before the measurements. Before and after drying the weight was measured. The skeletal volume ($V_{skeletal}$) of the plugs were measured with a Quantachrome Pentapyc 5200e (PPY-30 T) pycnometer. He-porosity (φ_{He}) can be calculated from the data of $V_{skeletal}$ and V_{med}. Skeletal density ($\rho_{skeletal}$) and bulk density (ρ_{bulk}) were also determined.

Table 1. *Number of prepared and analysed samples from different boreholes*

Sample type	BAF-1,-1A	BAF-2	Alpha	BAF-ib4	Covering sandstone
Axial	7	14	7	22 + (10)*	4
Horizontal	14	28		6 + (14)*	4
Fragment	7	15	2	55	8

*Plugs with 2.54 mm diameter.

Downloaded from http://sp.lyellcollection.org/ by guest on December 10, 2018

The N_2 (77 K) and CO_2 (273 K) adsorption–desorption isotherms were measured on fragments and 9 mm diameter samples by the Quantachrome Autosorb AS-1 surface area and pore size analyser. The samples were outgassed under vacuum at 105°C after the drying process. In the case of N_2 gas, BET surface area (S_{BET}), total pore volume (V_{tot}), pore size distribution (BJH method) and fractal dimension (D_F) with FHH method (Avnir & Jaroniec 1989) were calculated. The total pore volume is derived from the amount of vapour adsorbed at the highest relative pressure, by assuming that the pores are then filled with liquid adsorbate. The maximum relative pressure value during the tests was 0.9941, which is about 320 nm pore diameter (d_{max}). Micropore volume (V_{mic}) and micropore surface area (S_{mic}) were calculated according to the Dubinin-Radushkevich method from the CO_2 isotherms. Following the physisorption tests, the Hg-porosimetry measurements were carried out on the same samples by the Quantachrome Poremaster-60 GT instrument. The maximum (420 MPa) and minimum (1.5 kPa) applied pressure correspond to 3 nm and 800 µm pore throat diameter according to the Washburn equation (Lowell *et al.* 2004), respectively. The contact angle values were measured by the Quantachrome contact anglometer and 485.5 erg cm^{-2} (485.5 mN m^{-1}) surface tension value was used during the calculation. Pore throat size distribution in meso- and macropore region, Hg-porosity (φ_{Hg}), specific surface area (S_{Hg}) and fractal dimension (D_Z) by the Zhang method (Zhang *et al.* 2006) were calculated during the tests. The fractal dimension is related to the surface roughness, which value is two in the case of a smooth surface and three on a complex, very rough surface.

Ultrasonic pulse-transmission technique (ASTM 2008) was used to determine the P- and S-wave velocities. Travel times for velocity data were determined with a 'first-break' detection (Fig. 7) using a modified Akaike Information Criteria algorithm (Akaike 1973; Koroncz & Fedor 2016). The frequency of the transducers used for measurements was centred around 1 MHz, both for compressional and shear waves. The measurements were carried out on air-dried samples at room-temperature condition in a high-pressure triaxial cell. The applied confining pressures were calculated from corrected density-log data depending on the depth of origin of the samples.

In the case of the BCF only the pressure pulse decay (PPD) method was applicable for permeability measurements. From the early 2000s a new reservoir state PPD permeameter was developed and applied for this purpose, which allows fast and repeatable measurements of very tight rocks (Fedor 2011*a*, *b*, 2014). Conditions of measurements (pressure, temperature) are estimated from geophysical and hydrogeological surveys. First, air dry gas permeability was measured, followed by saturation with ultra-pure water and water permeability measured in reservoir conditions, and finally the dry-state permeability was measured on a given plug.

Results

The tested plugs show low φ_{He}, in the case of covering sandstone and the BAF-1, -1A samples, and greater differences were found that is indicating anisotropy (Table 2).

The adsorption–desorption isotherms can be classified to the type IV according to the IUPAC classification. Hysteresis can be observed on all isotherms due to the capillary condensation (Groen *et al.* 2003), but shapes of the loops are different. The loop of BAF-Ib-4 and BAF-2 samples is difficult to categorize but has a similar shape to the H2(b) type (Fig. 5). Complex pore structure and network effects belong to H2 type hysteresis loop. Within this type the H2(b) is associated with the pore blocking effect caused by pore neck, where the size distribution of neck widths is in wide range (Thommes *et al.* 2015). The hysteresis loop of the BAF-1, -1A and covering sandstone samples can be categorized into the H3 type (Fig. 6) which is typical for the slit-like pore materials (Condon 2006). According to the pore size distribution the BAF-Ib-4 and BAF-2 samples show peaks below 10 nm. Peaks can be found below 100 nm in the case of covering sandstone that suggests macropores besides the mesopores. The V_{mic} and S_{mic} results calculated from CO_2 isotherms confirm that all samples have also micropores (Table 3). The physisorption measurements made with CO_2 gas at 273 K give more realistic results to the V_{mic} and S_{mic}. At elevated temperature and under higher absolute pressure CO_2 molecules can more easily access micropores than N_2 at 77 K (Cazorla-Amoros *et al.* 1996) It should be noted that the adsorption and desorption branches of N_2 isotherms are not closed in the case of six BAF-2 samples. This means incomplete equilibration due to slow diffusion in small micropores that resulted in restricted access to wider pores through this small micropores. Two fractal ranges were found on the adsorption branch at a relative pressure 0.10–0.43 and 0.50–0.90 with D_{F1} and D_{F2} fractal dimension values. According to the investigation on coal, the D_{F1} reflects the pore surface fractal dimension and D_{F2} relates to the pore structure fractal dimension (Yao *et al.* 2008). The values of D_{F1} and D_{F2} are in the ranges 2.552–2.660 and 2.726–2.762 respectively, which indicates that the pore surface and pore structure of the samples are heterogeneous. In every case $D_{F2} > D_{F1}$, which means that the pore structure is more complicated than pore surface (Li *et al.* 2016). According to the BAF-Ib-4 and



Fig. 7. A typical automatic detection of first break in case of shear waves.

Downloaded from http://sp.lyellcollection.org/ by guest on December 10, 2018

Downloaded from http://sp.lyellcollection.org/ by guest on December 10, 2018

Table 2. *Calculated parameters obtained by He-pycnometry*

Parameters		BAF-1, -1A	BAF-2	BAF-Ib-4	Covering sandstone
$\rho_{skeletal}$ (g cm^{-3})	All samples	2.729 ± 0.039	2.737 ± 0.018	2.655 ± 0.056	2.655 ± 0.007
	Axial	2.739 ± 0.058	2.733 ± 0.014	2.653 ± 0.061	2.656 ± 0.007
	Horizontal	2.723 ± 0.027	2.739 ± 0.019	2.661 ± 0.045	2.654 ± 0.007
ρ_{bulk} (g cm^{-3})	All samples	2.644 ± 0.051	2.697 ± 0.019	2.603 ± 0.051	2.525 ± 0.015
	Axial	2.641 ± 0.056	2.693 ± 0.014	2.601 ± 0.055	2.522 ± 0.020
	Horizontal	2.646 ± 0.051	2.699 ± 0.020	2.608 ± 0.045	2.528 ± 0.009
φ_{He} (%)	All samples	3.09 ± 1.87	1.46 ± 0.39	2.14 ± 1.15	4.91 ± 0.70
	Axial	3.55 ± 2.83	1.46 ± 0.31	2.26 ± 1.30	5.06 ± 0.98
	Horizontal	2.86 ± 1.22	1.47 ± 0.43	1.95 ± 0.79	4.77 ± 0.35

BAF-2 Hg-porosimetry data, small amounts of mercury was intruded below 20 nm in the mesopore region (Table 4). The covering sandstone samples show peaks in the 0.1–5 μm diameter range and also below 50 nm, while in the case of BAF-1, -1A intrusion was found typically in the 5–50 μm diameter range. So, these samples show macropore characteristics too. In all cases the φ_{Hg} values were lower than those from He-pycnometry. This can be explained by the fact that helium gas can also fill pores and cracks with 0.25 nm diameter, while mercury cannot be injected into the pores with diameter less than 3 nm. This also suggests that the pore structure of the samples contain micropores. The fractal dimension calculated with the Zhang method can only be interpreted typically in 70–240 μm diameter range. Thus, the calculated values are likely to be related to the sample surface but are not in connection with the pore structure. In the case of BAF-1, 1A and BAF-2, however, mercury injection was observed only with five fragment samples.

Water permeability values were very low in all samples in the micro or nano Darcy range (10^{-19}–10^{-22} m^2). The distribution of gas permeability values measured on the same samples show a scattering over a large scale and they were 2–6 order of magnitudes higher than water permeability values that indicate the effect of drying. While the difference between water and gas permeability is about 2–3 order of magnitudes higher on the BAF-2 plugs on average (maximum and minimum values were 10^{-16} and 10^{-20} m^2), in the case of the BAF-1, -1A plugs this value is between 5 and 6 (maximum and minimum values were 10^{-13} and 10^{-19} m^2). The reason for this phenomenon is the reopening/opening of cracks due to drying (water loss of clay minerals). Moreover, a slight anisotropy could be observed, which indicates micro layering. Compared to plugs from the Alpha-tunnel (Fedor *et al.* 2008) and the Ib-4 borehole, the following differences and similarities could be recognized: six plugs from three delta cores from the Alpha-tunnel were measured and the water and gas permeability were between 10^{-20}–10^{-21} m^2 and 10^{-18}–10^{-19} m^2, respectively. After more than 50 different plugs from the Ib-4 borehole, the water permeability was between 10^{-17} and 10^{-21} m^2 and gas permeabilities were 10^{-16} and 10^{-22} m^2 on average, but extremely small pico Darcy scale permeability on the reservoir state was measured, too.

Results of compressional and shear wave velocity measurements are shown in Tables 5 and 6, and Figure 8 respectively. Test results indicated that the BCF can be characterized by higher velocities than the covering sandstone formations.

Porewater characterization of the BCF: preliminary results

On the basis of pore structure and reservoir characterization, it can be concluded that the main water and solute transport process is molecular diffusion in BCF. The swelling clay content basically influences the self-healing and most cracks are closed under reservoir conditions. Permeability depends particularly on pore-size distribution, clay mineral quality and quantity, pressure and temperature and indirectly depends on porewater salinity and dissolved gas content in the porewater. Darcy's definition of permeability in this range is not valid (i.e. non-laminar flow, effect of compressibility, reaction transport processes, temperature dependence of viscosity, etc.). Water permeability measured by PPD cannot be compared by Klinkenberg permeability calculated from gas permeability and comparability of PPD, as pressure fall-off or steady-state gas permeability values are limited. The water composition of opened cracks and water of pores are presumably different, and only limited interaction could be observed at a molecular level. Hence, the water enclosed in capillaries is in a near equilibrium state both with rock and free porewater. The age of closure and original composition of water is not yet known.

Downloaded from http://sp.lyellcollection.org/ by guest on December 10, 2018

Table 3. *Calculated parameters from the physisorption analysis*

Samples	N_2						CO_2	
	S_{BET} ($m^2\ g^{-1}$)	V_{tot} (d_{max} = 320 nm) ($cm^3\ g^{-1}$)	Fractal dimension				V_{mic} ($cm^3\ g^{-1}$)	S_{mic} ($m^2\ g^{-1}$)
			Relative pressure range (−)	D_{F1} (−)	Relative pressure range (−)	D_{F2} (−)		
BAF-Ib-4	16.30 ± 2.30	1.85E-02 ± 1.31E-03	0.10–0.43	2.596 ± 0.030	0.48–0.85	2.748 ± 0.021	5.11E-03 ± 5.57E-04	14.66 ± 2.17
Covering sandstone	5.45 ± 0.89	9.75E-03 ± 7.39E-04	0.10–0.41	2.552 ± 0.034	0.46–0.91	2.726 ± 0.020	1.37E-03 ± 2.19-04	3.92 ± 0.63
BAF-2	7.95 ± 2.80	8.41E-03 ± 2.00E-03	0.12–0.43	2.598 ± 0.049	0.49–0.78*	2.762 ± 0.038*	2.84E-03 ± 1.13E-03	9.36 ± 2.88
BAF-1, -1A	3.02 ± 1.32	5.37E-03 ± 1.97E-03	0.10–0.41*	2.660 ± 0.013*	0.50–0.87*	2.754 ± 0.011*	1.35E-03 ± 3.71E-04	3.88 ± 1.07

*Only five measurements can be interpreted in this relative pressure range.

Downloaded from http://sp.lyellcollection.org/ by guest on December 10, 2018

Table 4. *Calculated parameters from Hg-porosimetry*

Parameters	Contact angle (°)	φ_{Hg} (%)	S_{Hg} ($m^2\ g^{-1}$)	D_Z (–)
BAF-ib4	144.59 ± 1.09	1.82 ± 0.47	4.08 ± 1.00	2.560 ± 0.041
Covering sandstone	139.03 ± 1.53	2.44 ± 0.53	0.50–1.50	2.645 ± 0.021
BAF-2	155.43 ± 3.05	0.78 ± 0.44* (0.68)†	2.07 ± 1.08* (1.87)†	2.697 ± 0.068*
BAF-1, -1A	157.67 ± 5.85	1.53 ± 0.76 (1.18)†	0.20–2.00	2.661 ± 0.074

*Only five measurements can be interpreted.
†Due to the high standard deviation value median value is also indicated.

During core drilling the rock is released through stress and some significant cracks could be re-opened. The surface of the core and these cracks could be washed by the drilling fluid and possibly damaged, but the inner parts of the BCF cores were unchanged because of the pore size. Presumably, the effect of pollution spread very slowly towards the inner area as some isotope transport experiments showed (Lakatos *et al.* 2002; Lázár *et al.* 2008). Depending on the circumstances of storage, higher pores could partly lose their water, but on the basis of experiments, a higher temperature is needed to open meso and micropores, they being less sensitive to the external environment. This is the reason why older BCF cores can also be used for experiments, and it has been observed that the rock can adsorb the humidity of a human hand or air after drying. During this time, the water content of pores will change in the macropores and slowly change at the meso- and micropores. Therefore, two factors have to be handled during the sampling and preparation of experiments regarding the reliable porewater analysis. On the one hand, it is important to design a fast and clear sampling technique *in situ*. On the other hand, the pollution of core samples before measurement has to be avoided during the plugging and sample handling.

In-situ *sampling for water content analysis*

The process of *in-situ* sampling from the borehole was as follows. After pulling out the core it was washed with ultra-pure water (removing contaminants) and the drilling direction was marked with a scratch. This was followed by a fast, geological description and photo documentation in the field. Afterwards an *c.* 1 m-long core was put into an aluminium core holder, the weight of which was known, and closed. This core holder was put under vacuum and pressurized with high purity helium. From

Table 5. *Results of compressional wave velocity measurements*

Samples	Sample size	Material	Median ($m\ s^{-1}$)	Min ($m\ s^{-1}$)	Max ($m\ s^{-1}$)
BAF-1/1A	17	Sandstones and conglomerates	4085	3282	4689
BAF-2	39	Claystone	5035	3868	5574
Delta-3	2	Claystone	–	5435	5557
Ib-4	3	Claystone	4980	4701	5518

Table 6. *Results of shear wave velocity measurements*

Samples	Sample size	Material	Media [$m\ s^{-1}$]	Min [$m\ s^{-1}$]	Max [$m\ s^{-1}$]
BAF-1/1A	17	Sandstones and conglomerates	2731	1711	3117
BAF-2	39	Claystone	2923	2048	3297
Delta-3	2	Claystone	–	3051	3052
Ib-4	3	Claystone	3112	2951	3297

Downloaded from http://sp.lyellcollection.org/ by guest on December 10, 2018

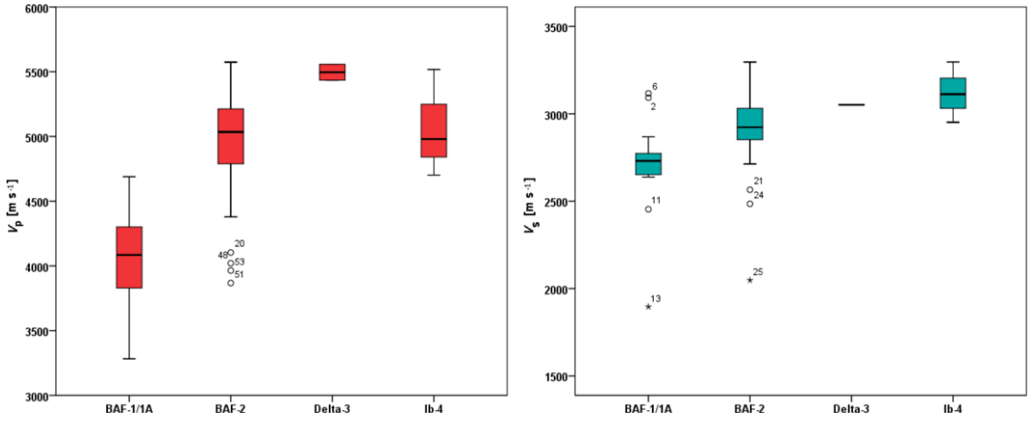


Fig. 8. Test results of compressional (V_p) and shear (V_s) wave velocities from different locations.

time to time the pressure had to be checked. After 3 years a 2.5 bar pressure drop was observed in the first two samples which were taken from borehole BAF-2 (808.87–809.8 m, 836.58–837.42 m) and were stored at room temperature (between 15°C and 25°C). One sample was given to the OECD/NEA Clay Club CLAYWAT project (in progress) and another one was stored for later analysis when the methodology and technology are ready.

Possible porewater extraction technology in the case of the BCF

There are many different methods to extract porewater from rocks (i.e. low- or high-speed centrifugation, displacement by immiscible liquids, aqueous leaching technique, squeezing technique, azeotropic, vacuum or microdistillation, direct equilibration with water or CO_2, radial diffusion or diffusive exchange, lyophilization (cryodesiccation), etc.). A good summary of applied technologies can be found in Sacchi *et al.* (2000) and Weaver (2014). Unfortunately, only some of them were tried in the case of BCF and the validity of the results is questionable. Within the framework of the EU-financed FUNMIG project (2005–8) the RTDC3 subproject investigated the porewater composition of clayey rocks (Fernández *et al.* 2009). Some samples from the Ib-4 and the Alpha-tunnel were analysed for isotope transport, microaudiography, microtomography, XRD, FTIR, TGA, SEM, IEC and porewater content. Marques (2011) and Marques *et al.* (2012) analysed the porewater of BCF by direct equilibration with water but the results are questionable because of prerequisites. The squeezing technology was also tried but failed in the case of the BCF due to the high pressures required for this type of rock (Fernández *et al.* 2009).

As a preliminary experiment, a modified cryodesiccation (LN2 freezing) was carried out on two samples from the Alpha-tunnel in the GEOCHEM Laboratory. Cryodesiccation (lyophilization) is a process which applies solid CO_2 and is used in the food industry for making deep-frozen products. The original technology is not applicable in the case of BCF because only CO_2 sublimates and distilled water can be extracted. The new process was the following (Fig. 9): first, a well-defined and dried sample was inserted into a pressurizable core holder and flooded with liquid N_2 and then closed. A short time later the frozen sample was heated up to 105°C and afterwards cooled with liquid N_2 again. This process was repeated 2–3 times. Dried, porewater free samples have to be used because of the long storage of the investigated core (Delta-3) and hence the possible chemical changes in mobile, free porewater. In this case only capillary trapped water has to be used which is irreducible in normal circumstances. In case of intact cores free porewater also has to be used for water chemical analysis.

The aim of this experiment was that initially the porewater would freeze in capillaries and the volume of porewater would increase. It is crucial that all opened dry pores have to be flooded by liquid N_2. Due to heating the N_2 expands and dissolves in the porewater. In the next period the water was frozen again and during the next heating gaseous N_2 expanded in the capillaries. Finally, the water in the capillaries was displaced by N_2. From a *c.* 70 cm^3 plug, about 1.5–2 ml of water was extracted and analysed. The preliminary results of the water chemical analysis are given in Table 7.

Unfortunately, the sample size was too small for a full chemical analysis, but the experiment results show chemically non-distilled water. It is very important to emphasize that these are only the

Downloaded from http://sp.lyellcollection.org/ by guest on December 10, 2018

Table 7. *Preliminary results of water chemical analysis of the BCF obtained by a modified cryodesiccation (LN_2 freezing) method*

Fluoride	Chloride	Nitrite	Nitrate	Bromide	Phosphate	Sulphate
mg l^{-1}	mg l^{-1}	mg l^{-1}	mg l^{-1}	mg l^{-1}	mg l^{-1}	mg l^{-1}
<10	539	<10	304	<10	<50	105
Li	Be	B10	Al	V	Cr	Mn
µg l^{-1}	µg l^{-1}	µg l^{-1}	µg l^{-1}	µg l^{-1}	µg l^{-1}	µg l^{-1}
2055.67	0.68	3592.11	21.00	4.80	151.48	4495.74
Co	Ni62	Cu63	Zn66	Fe54	As	Se80
µg l^{-1}	µg l^{-1}	µg l^{-1}	µg l^{-1}	µg l^{-1}	µg l^{-1}	µg l^{-1}
194.32	722.99	141.67	705.35	597.34	11.72	8.58
Rb	Sr	Mo sum (95)	Ag sum (107)	Cd111	Cs	Ba135
µg l^{-1}	µg l^{-1}	µg l^{-1}	µg l^{-1}	µg l^{-1}	µg l^{-1}	µg l^{-1}
23.12	530.01	59.13	6.24	<2	0.36	211.86
La	Tl sum (205)	Pb sum	Bi	Th	U238	Sn
µg l^{-1}	µg l^{-1}	µg l^{-1}	µg l^{-1}	µg l^{-1}	µg l^{-1}	µg l^{-1}
0.71	<2	4.01	12.78	7.79	<5	117.00
Hg	Sb					
µg l^{-1}	µg l^{-1}					
–	16.80					

preliminary results of two experiments. A more special sampling will be implemented with core samples from the next BCF borehole, a more undisturbed sample being investigated in the same way. Several other technologies, such as aqueous leaching (Bradbury & Baeyens 1998; Sacchi *et al*. 2000; De Craen M. *et al.* 2004), might be used and compared with N_2 freezing results.

Summary and conclusions

BCF is a very tight, clayey rock with extremely low porosity and permeability, nano size pores and a small content of swelling clay mineral. Although the mineralogy and petrology of this formation is relatively well defined, measurements of rock mechanical, petrophysical and hydrodynamic parameters are a real challenge.

On the basis of recent research and development of the past few years the process of sedimentation of different blocks could be reconstructed.

Equipment and methodological developments were needed for the investigation of the reservoir geological and hydrodynamic behaviour of this rock: these have been ongoing since the early 2000s.

Pore characterization experiments show complex pore structure. According to the pore size distribution, the BAF-Ib-4 and BAF-2 samples (real BCF) show peaks below 10 nm and relatively small pore surface and volume. Peaks can be found below 100 nm in the case of covering sandstone, which suggests macropores besides the mesopores. Fractal dimensions could be calculated and used for characterizing the pore surface and structure.

On the basis of petrophysical experiments, the real BCF is characterized by very low porosity and water permeability, which is 2–3 times higher than the gas permeability. Tight, highly consolidated rock mechanical character could be observed on the basis of acoustic measurements. The main transport process is diffusion.

Traditional water extraction methods are not adaptable in this case because of the excessively low porosity and nano-scale pore size distribution, and hence, new cryodesiccation technology should be attempted. More experimentation is needed to confirm the results, and liquid equilibrium experiments are required to validate them.

Downloaded from http://sp.lyellcollection.org/ by guest on December 10, 2018



Fig. 9. BCF porewater extraction experiment: modified cryodesiccation (LN_2 freezing) method.

Downloaded from http://sp.lyellcollection.org/ by guest on December 10, 2018

Acknowledgments The authors would like to thank PURAM for all the data he provided and Gyula Konrád for his permission to use Figs 1, 2, and 3 in this article.

Funding This research received no specific grant from any funding agency in the public, commercial, or not-for-profit sectors.

References

Ács, P. & Fedor, F. 2015. Pore structure of Boda Claystone Formation, W-Mecsek, Hungary. *6th International Meeting on Clays in Natural and Engineered Barriers for Radioactive Waste Confinement*, 23–26 March 2015, Brussels, Belgium. [abstract]

Akaike, H. 1973. Information theory and an extension of the maximum likelihood principle. *In*: Petrov, B.N. & Csaki, F. (eds) *Second International Symposium on Information Theory*. Academiai Kiado, Budapest, 267–281.

Árkai, P., Balogh, K., Demény, A., Fórizs, I., Nagy, G. & Máthé, Z. 2000. Composition, diagenetic and post-diagenetic alterations of a possible radioactive waste repository site: the Boda Albitic Claystone Formation, southern Hungary. *Acta Geologica Hungarica*, **43/4**, 351–378.

ASTM 2008. *Standard Test Method for Laboratory Determination of Pulse Velocities and Ultrasonic Elastic Constants of Rock (D2845-08)*. ASTM International, West Conshohocken, PA.

Avnir, D. & Jaroniec, M. 1989. An isotherm equation for adsorption on fractal surfaces of heterogeneous porous materials. *Langmuir*, **5**, 1431–1433.

Barabás, A. & Barabás-Stuhl, Á. 1998. Stratigraphy of the Permian formations in the Mecsek Mountains and its surroundings. *In*: Bérczi, I. & Jámbor, Á. (eds) *Stratigraphy of Geological Formations of Hungary*. Mol Plc. and Hung. Geol. Institute, Budapest, 187–215 [in Hungarian].

Bradbury, M.H. & Baeyens, B. 1998. A physicochemical characterisation and geochemical modelling approach for determining pore water chemistries in argillaceous rocks. *Geochimica et Cosmochimica Acta*, **62/5**, 783–795.

Cazorla-Amoros, D., Alcaniz-Monje, J. & Linares-Solano, A. 1996. Characterization of activated carbon fibers by CO2 adsorption. *Langmuir*, **12**, 2820–2824.

Condon, J.B. 2006. *Surface Area and Porosity Determinations by Physisorption: Measurement and Theory*. Elsevier, San Diego.

Csicsák, J. (ed.) 1999. *The Short-Term Program for the Qualification of Boda Claystone Formation*, Research final report, V. volume, Hydrogeological, hydrochemical investigation program. MECSEKÉRC Inc., Pécs [in Hungarian].

De Craen, M., Wang, L., Van Geet, M. & Moors, H. 2004. The geochemistry of Boom Clay pore water at the Mol site, status 2004. SCK • CEN Scientific Report. BLG-990.

English, P.M. 2001. Formation of analcime and moganite at Lake Lewis, central Australia: significance of groundwater evolution in diagenezis. *Sedimentary Geology*, **143**, 219–244.

Fedor, F. (ed.) 2011*a*. *Summary report on 'Special Rock Physics and Geophysical Examinations to Compare the Laboratory and Field Measurements' project*. Mecsekérc Zrt. [in Hungarian].

Fedor, F. 2011*b*. The Importance of Laboratorial Petrophysical Characterization: possibilities and Limitations. *Hungarian Mining and Metallurgical Association: The First Central and Eastern European International Oil and Gas Conference and Exhibition*, Siófok.

Fedor, F. (ed.) 2013. *The complex investigation series on samples from the Ib-4 borehole*, Research report [Hungarian].

Fedor, F. (ed.) 2014. *Final report on GOP-1.3.1-11/A-2011-0098 project, 'Preparation of a Complex Transport Model and its Application in West Mecsek'*, Mecsekérc Zrt. [in Hungarian].

Fedor, F. & Somodi, G. 2010. Interdisciplinary investigation of the Boda Claystone Formation – geological scale and petrophysical properties. *In*: Pál-Molnár, E. (ed.) *Basin Development and Geological Resources*. Geolitera, Szeged, 49–51 [Hungarian abstract].

Fedor, F., Máthé, Z., Hámos, G., Somodi, G., Jobbik, A. & Szűcs, I. 2008. Laboratory pressure pulse decay permeability measurement of Boda Claystone, Mecsek Mts., SW Hungary. *Physics and Chemistry of the Earth, Parts A, B & C*, **33**, S45–S53.

Fedor, F., Fancsik, T. *et al.* 2012. Interdisciplinary investigation of Boda Claystone Formation – preliminary results. *5th International Meeting on Clays in Natural and Engineered Barriers for Radioactive Waste Confinement*, 22–25 October 2012, Montpellier, France. [poster presentation]

Fedor, F., Ács, P., Horváth, J., Koroncz, P. & Nagy, Gy. 2014. *Determination of the BCF pore water content – possibilities and limitations*, Research Report [in Hungarian].

Fedor, F., Máthé, Z., Koroncz, P. & Ács, P. 2016. Results of mineralogical, petrological, geochemical and petrophysical laboratory measurements carried out on samples of BAF-2 and BAF-1,-1A drillholes. *In*: Dályay, V. & Hámos, G. (eds) *BCF Research – Workshop*. Molnár Nyomda és Kiadó, Pécs, 52–62 [in Hungarian].

Fedor, F., Feuer, V. & Schön, R. 2017. How to automate a petrophysical laboratory? – challenges and solutions. *In*: Hatvani, I.G., Tanos, P., Cvetkovic, M. & Fedor, F. (eds) *Geomathematics in Multidisciplinary Science – The New Frontier?* Pécs Regional Committee of the Hungarian Academy of Sciences, 167–174.

Fernández, A.M., Melón, A. *et al.* 2009. Study of different Argillaceuos Formations performed in the context of the FUNMIG Project: Pore water chemistry and physical, mineralogical and geochemical properties in Boom Clay, Callovo-Oxfordian, Opalinus Clay and Boda Claystone rock samples. Technical Report Enresa 05/2009.

Groen, J.C., Peffer, L.A.A. & Pérez-Ramírez, J. 2003. Pore size determination in modified micro- and mesoporous materials. Pitfalls andlimitations in gas adsorption data analysis. *Microporous and Mesoporous Materials*, **60**, 1–17.

Haas, J. & Péró, Cs. 2004. Mesosoic evolution of the Tisza Mega-unit. *International Journal of Earth Sciences*, **93**, 297–313.

Downloaded from http://sp.lyellcollection.org/ by guest on December 10, 2018

JÁMBOR, Á. 1964. *Lower Permian Formations of the Mecsek Mountains*. Mecsek Ore Environment Company, Pécs [in Hungarian].

KONRÁD, GY. 2013. *General Geological Sections for the Comparison of Lithostratigraphic Units in the Boda and in the Gorica Blocks*. PURAM, Budaörs.

KONRÁD, GY., SEBE, K., HALÁSZ, A. & BABINSZKI, E. 2010. Sedimentology of a Permian playa lake: the Boda Claystone Formation, Hungary. *Geologos*, **16**, 27–41.

KORONCZ, P. & FEDOR, F. 2016. Experimental investigation of stress-dependent petrophysical behaviour of reservoir rocks. *In*: CVETKOVIC, M., NOVAK-ZELENIKA, K., HORVÁTH, J. & HATVANI, I.G. (eds) *Geomathematics – Present and Future of Geological Modelling*. Croatian Geological Society, 83–87.

KORONCZ, P., ÁCS, P., LEMBERKOVICS, V. & FEDOR, F. 2017. Pore characterization, acoustic and permeability measurements on core plug triplets, Miocene Tótkomlós (Calcareous Marl) Formation of the Pannonian-basin, Hungary. *Geologia Croatica*, **70/2**, 87–92.

KOVÁCS, L. (ed.) 1999*a*. *Digest on the Results of the Short-Term Characterization Programme of the Boda Claystone Formation*. PURAM-Mecsekérc.

KOVÁCS, L. (ed.) 1999*b*. *The Short-Term Program for the Qualification of Boda Claystone Formation*, Research final report [in Hungarian].

LAKATOS, I., FEDOR, F. & TÓTH, J. 2002. *Hydrodynamic Investigations on Samples from the Boda Claystone Formation*. Mecsekérc Plc. [in Hungarian].

LÁZÁR, K. & MÁTHÉ, Z. 2012. Claystone as a potetial host rock for nuclear waste storage. *In*: VALAŠKOVA, M. & MARTYNKOVA, G.S. (eds) *'Clay Minerals in Nature – Their Characterization, Modification and Application'*. IntechOpen, London, 55–80. https://doi.org/10.5772/48123

LÁZÁR, K., MEGYERI, J., PARNEIX, J.-C., MÁTHÉ, Z. & SZARVAS, T. 2008. Diffusion rate of anion species (99TcO4 -, H14CO3-) and HTO in Boda Claystone borehole samples. *4th. Annual Workshop Proceedings 6TH EC FP – FUNMIG IP*, 24–27 November 2008, Karlsruhe.

LI, A., DING, W., HE, J., DAI, P., YIN, S. & XIE, F. 2016. Investigation of pore structure and fractal characteristics of organic-rich shale reservoir: a case study of Lower Qiongzhusi formation in Malong block of eastern Yunnan Province, South China. *Marine and Petroleum Geology*, **70**, 46–57.

LOWELL, S., SHIELDS, J.E., THOMAS, M.A. & THOMMES, M. 2004. *Characterization of Porous Solids and Powders: Surface Area, Pore Size and Density*. Particle Technology Series, **16**, Springer, Netherlands.

LOWENSTEIN, T.K. & HARDIE, L.A. 1985. Criteria for recognition of salt-pan evaporites. *Sedimentology*, **32**, 627–644.

MARQUES, F.M., VER, N. & BAEYENS, B. 2012. Application of the 'bottom up' approach for the predictive modelling of sorption isotherms on Hungarian Boda Clay. *5th International Meeting on Clays in Natural and Engineered Barriers for Radioactive Waste Confinement*, 22–25 October 2012, Montpellier, France. [poster]

MARQUES, M. 2011. Paul Scherrer Institut, Laboratory for Waste Management *WP 2: Macroscopic sorption investigations on argillaceous rocks*, PSI.

MÁTHÉ, Z. (ed.) 1998. *Summary Report of the Site Charachterization Program of the Boda Siltstone Formation*, **4**. Mecsek Ore Environment Company, Pécs [in Hungarian].

MÁTHÉ, Z. 2015. *Results of mineralogical, petrological and geochemical investigation of Boda Claystone Formation*. PhD thesis, ELTE Department of Petrology and Geology, Budapest [in Hungarian].

MÁTHÉ, Z. & VARGA, A. 2012. 'Seasoning' to the palaeoenvironmental reconstruction of the Permian Boda claystone Formation: pseudomorphs after halit int he claystone samples of the deep drillings BAT-4. *Bulletin of the Hungarian Geological Society*, **142/2**, 201–204.

MÉV 1993. *Report about the results of geological research related to the recommended Mecsek Deep Waste Disposal Site in 1989–1992*. Hungarian research report. (MÉV, Pécs). MÉV Database.

NÉMETH, T., MÁTHÉ, Z. *ET AL.* 2016. Clay minerology of the Boda Claystone Formation (Mecsek Mts., SW Hungary). *Open Geoscience*, **8**, 259–274, https://doi.org/10.1515/geo-2016-0024

REMMY, R.R. & FERRELL, R.E. 1989. Distribution and origin of analcime in marginal lacustrine mudstones of the Green River Formation, south-central Uinta Basin, Utah. *Clays and Clay Minerals*, **37**, 419–432.

ROY, P.D., SMYKATZ-KLOSS, W. & SINHA, R. 2006. Late Holocene geochemical history inferred from Sambhar and Didwana playa sediments, Thar Desert, India: comparison and synthesis. *Quaternary International*, **144**, 84–98.

SACCHI, E., MICHELOT, J.L. & PITSCH, H. 2000. *Pore-Water Extraction from Argillaceous Rocks for Geochemical Characterisation: Methods and Interpretations*. OECD Publications, Paris.

SIPOS, P., NÉMETH, T. & MÁTHÉ, Z. 2010. Preliminary results on the Co, Sr, and Cs sorption properties of the analcime-containing rock type of the Boda Siltstone Formation. *Central European Geology*, **53/1**, 67–78, https://doi.org/10.1556/CEuGeol.53.2010.1.4

SZKFI 1990. *Determination of the permeability of Lower Permian BCF samples by constant reservoir pressure at changing pore pressure and temperature*, Hungarian Hydrocarbon Institute report, Nagykanizsa [in Hungarian].

SZKFI 1991. *Determination of the permeability of Lower Permian BCF samples by constant reservoir pressure at changing pore pressure and temperature*, Hungarian Hydrocarbon Institute, part of report, Nagykanizsa, 1991 [in Hungarian].

SZŰCS, I. & FEDOR, F. 2007. Spatial extension and parameter integration into the safety case – examples from the Hungarian LLW/ILW and HLW disposal project. *Linkage of Geoscientific Arguments and Evidence in Supporting Safety Case (Workshop Proceedings)*, OECD NEA No. 6119, 163–165.

THOMMES, M., KANEKO, K., NEIMARK, A.V., OLIVIER, J.P., RODRIGUEZ-REINOSO, F., ROUQUEROL, J. & SING, K.S.W. 2015. Physisorption of gases, with special reference to the evaluation of surface area and pore size distribution (IUPAC Technical Report). *Pure Applied Chemistry*, **85**, 1051–1069.

VARGA, A., SZAKMÁNY, GY., RAUCSIK, B. & MÁTHÉ, Z. 2005. Chemical composition, provenance and early diagenetic processes of playa lake deposits from

Downloaded from http://sp.lyellcollection.org/ by guest on December 10, 2018

the Boda Siltstone Formation (Upper Permian), SW Hungary. *Acta Geologica Hungarica*, **48**, 49–68.

VARGA, A., RAUCSIK, B., SZAKMÁNY, Gy. & MÁTHÉ, Z. 2006. Mineralogical, petrological and geochemical characteristics of the siliciclastic rock types of Boda Siltstone Formation. *Bulletin of the Hungarian Geological Society*, **136/2**, 201–232.

WEAVER, C.B. 2014. *'Pore Water Extraction for Unsaturated Zone Isotope Research: An Investigation using an Immiscible Displacement Fluid and a Centrifuge'*. Dissertations & Theses in Earth and Atmospheric Sciences. Paper 48, http://digitalcommons.unl.edu/geoscidiss/48

YAO, Y., LIU, D., TANG, D., TANG, S. & HUANG, W. 2008. Fractal characterization of adsorption-pores of coals from North China: an investigation on CH 4 adsorption capacity of coals. *International Journal of Coal Geology*, **73**, 27–42.

ZHANG, B., LIU, W. & LIU, X. 2006. Scale-dependent nature of the surface fractal dimension for bi- and multi-disperse porous solids by mercury porosimetry. *Applied Surface Science*, **253**, 1349–1355.